

THE MATMOD APPROACH TO MODELLING  
OF ZIRCALOY NON-ELASTIC DEFORMATION\*

Alan K. Miller  
Department of Materials Science and Engineering  
Stanford University

SUMMARY OF PRESENTATION

The MATMOD constitutive equations represent a unified model for the non-elastic deformation behavior of metals and alloys. The equations are, to some extent, a bridge between materials science and structural analysis: The overall form of the equations follows from the dislocation-controlled physical nature of most non-elastic deformation, but the actual expressions and materials constants are determined by fitting the mechanical test data. The equations are probably most useful in treating various mixed situations, such as creep-fatigue interaction, mixtures of thermal and irradiation creep, or interactions of strain hardening and recovery. They have been applied in detail to Zircaloy, to type 316 austenitic stainless steel, and to 2 1/4Cr-1Mo ferritic alloy steel.

As seen in Figure 1, the central MATMOD equation is one which expresses the non-elastic strain rate  $\dot{\epsilon}_{th}$  as a function of the current stress  $\sigma$  and temperature  $T$  and also as a function of four structure variables. The first two of these ( $F_{def}$  and  $R$ ) are history-dependent state variables which represent, respectively, the current states of isotropic and directional hardening. The second two structure variables ( $F_{sol,1}$  and  $F_{sol,2}$ ) are temperature and strain-rate dependent solute strength variables which represent, respectively, the effects of alloying elements which either do not or do interact synergistically with strain hardening. Each of the

\* Research on Zircaloy sponsored by EPRI (RP-456, RP-700); research on austenitic stainless steels and 2 1/4Cr-1Mo steel sponsored by U.S. Department of Energy (EY-76-S-03-0326PA57).

APS 2001

1605 293

four structure variables corresponds to a specific strengthening mechanism (Figure 1).

The fact that there is only one non-elastic strain variable for out-of-reactor situations (instead of the traditional separation into "creep" and "plastic" strains) leads to straightforward predictions of interactions between "creep" and "plasticity" (Figure 2) and between monotonic and cyclic deformation (Figure 3). Recovery effects are also predicted in a straightforward manner because both  $R$  and  $F_{def}$  are governed by work hardening-recovery type equations (Figure 4).

Dynamic strain aging effects such as (1) plateaus in the yield strength versus temperature curve (Figure 5), (2) a local minimum in the strain-rate sensitivity versus temperature curve (Figure 6), and variations with temperature in the slope of the creep rate versus stress curve (Figure 7) are simulated in a natural way through the solute strengthening variables  $F_{sol,1}$  and  $F_{sol,2}$ .

Irradiation effects have been added (to the above descriptions of out-of-reactor deformation) by (1) adding a neutron flux hardening term to the strain hardening term in the equation controlling  $F_{def}$ , and (2) by adding a steady-state irradiation creep rate to  $\dot{\epsilon}_{th}$ . With these additions, the equations make reasonable predictions of (1) the fluence dependence of the yield strength for both cold-worked and annealed Zircaloy (Figure 8) and (2) the creep-rate versus stress behavior obtained in-reactor, out-of-reactor, and post-irradiation (Figure 9).

Figures 10 and 11 compare the model's predictions against independent data for strain-rate change tests. For annealed and for CWSR materials the average errors in predicted stress are 8% and 17%, respectively. Figure 12 shows the stress relaxation behavior of the model; it compares

favorably against independent data over a 25°C to 500°C temperature range.

A major deficiency of the model, as applied to Zircaloy, has been the fact that the yield strength plateau, simulated in annealed material, is erased by cold work, leading to the inaccuracy shown in Figure 13. This deficiency has been rectified in recent modelling work on 316 stainless steel in which  $F_{sol,2}$  was introduced; Figure 14 shows how the latest equations can actually simulate an increase in dynamic strain aging effects with increasing cold work.

In summary, the MATMOD approach has the advantages of: (1) physical basis (useful for extrapolations) and (2) great breadth; Figure 15 lists the large number of phenomena covered by the model. The approach has the disadvantages of (1) less accuracy than special-purpose equations fitted to specific regimes of behavior and (2) a relatively difficult procedure for calculating the materials constants for other alloys.

A list of references on the MATMOD constitutive equations is attached.

1605 295

## REFERENCES ON THE MATMOD CONSTITUTIVE EQUATIONS

### PUBLICATIONS:

1. A. Miller, "An Inelastic Constitutive Model for Monotonic, Cyclic, and Creep Deformation," J. of Engg. Materials and Technology, 98-H, 97-113 (1976).
2. A. K. Miller, "Progress in Modelling of Zircaloy Non-Elastic Deformation Using a Unified Phenomenological Model," ASTM-STP-633 (1977).
3. A. K. Miller, "Predictions of Localized Plastic Flow Conditions in Irradiated Zircaloy Using a Unified Phenomenological Model," Fourth Intl. Conf. on Structural Mechanics in Reactor Technology, 1977, paper #C3/8.
4. A. K. Miller and C. F. Shih, "An Improved Method for Numerical Integration of Constitutive Equations of the Work Hardening-Recovery Type," J. of Engg. Materials and Technology, 99H, 275-277 (1977).
5. A. K. Miller and O. D. Sherby, "A Simplified Phenomenological Model for Non-Elastic Deformation: Predictions of Pure Aluminum Behavior and Incorporation of Solute Strengthening Effects," Acta Met., 26, 289-304 (1978).
6. S. Oldberg, Jr., A. K. Miller, and G. E. Lucas, "Advances in Understanding and Predicting Inelastic Deformation in Zircaloy," Zirconium in the Nuclear Industry (Stratford, England, 1978) to be published in ASTM STP.
7. A. K. Miller, "A Unified Approach to Predicting Interactions Among Creep, Cyclic Plasticity, and Recovery," Nuclear Engg. and Design, 51, 35-43 (1978).
8. O. D. Sherby and A. K. Miller, "Combining Phenomenology and Physics in Describing the High Temperature Mechanical Behavior of Crystalline Solids," Journal of Engineering Materials and Technology, in press, 1979.

### REPORTS:

1. A. K. Miller, "A Unified Phenomenological Model for the Monotonic, Cyclic, and Creep Behavior of Strongly Work-Hardening Materials," Ph.D. dissertation, Stanford University Department of Materials Science and Engineering, May 1975.
2. A. K. Miller and O. D. Sherby, "Development of the Materials Code, MATMOD (Constitutive Equations for Zircaloy)" EPRI final report #NP-567, Dec. 1977.
3. A. K. Miller and O. D. Sherby, "Modelling of Deformation and Fracture in High-Temperature Structural Materials," Progress Report for the period Sept. 1, 1977 to May 1, 1978, Stanford Univ. Dept. of Materials Sci. and Engg.
4. A. K. Miller and O. D. Sherby, "Modelling of Deformation and Fracture in High-Temperature Structural Materials," Progress report for the period May 1, 1978 to March 31, 1979, Stanford Univ. Dept. of Mat. Sci. and Engg.

1605 296

5. C. G. Schmidt, "Modularized Program for Integrating Constitutive Equations Describing Plastic Flow Using Simple Boundary Conditions," Stanford Univ. Dept. of Materials Science and Engg. Report # SU-DMS-78-T-4, June 1979
6. C. G. Schmidt, "A Unified Phenomenological Model of Solute Strengthening, Deformation Strengthening, and their Interactions in Type 316 Stainless Steel," Ph.D. dissertation, Stanford Univ. Dept. of Materials Science and Engg., Sept. 1979.

1605 297

1802 548

MATMOD CONSTITUTIVE EQUATIONS

I. General Form:

A. Thermal strain rate:

$$\dot{\epsilon}_{th} = f(T) f[ \sigma/E - R, F_{def}, F_{sol,1}, F_{sol,2} ]$$

B. History-dependent state variables:

1. R ("Rest stress" or back stress):

Directional (kinematic) hardening associated with pileups or dislocation bowing

2.  $F_{def}$  ("Friction stress due to deformation"):

Isotropic hardening associated with subgrains, forest dislocations, irradiation

$$\dot{R} = \frac{dR}{dt} = \begin{matrix} \text{work-hardening} \\ \text{term} \end{matrix} - \begin{matrix} \text{thermal recovery} \\ \text{term} \end{matrix}$$

$$\dot{F}_{def} = \frac{dF_{def}}{dt} = \begin{matrix} \text{work-hardening} \\ \text{term} \end{matrix} + \begin{matrix} \text{flux-hardening} \\ \text{term} \end{matrix} - \begin{matrix} \text{thermal recovery} \\ \text{term} \end{matrix}$$

C. Temperature and strain-rate dependent solute strengthening variables:

$F_{sol}$  ("Friction stress due to solutes"):

Isotropic strengthening associated with solute atmospheres, dynamic strain aging, etc.

$$F_{sol} = f(T, \dot{\epsilon})$$

1.  $F_{sol,1}$  : independent of strain hardening (substitutional solutes?)

2.  $F_{sol,2}$  : synergistic with strain hardening (interstitial solutes?)

II. Specific Equations (1-dimensional form):

$$\dot{\epsilon}_{th} = B\theta' \left\{ \sinh \left[ \left( \frac{|\sigma/E - R|}{\sqrt{F_{sol,1} + F_{def}(1+F_{sol,2})}} \right)^{1.5} \right] \right\}^n \text{sgn}(\sigma/E - R) \quad (1)$$

$$\dot{R} = H_1 \dot{\epsilon}_{th} - H_1 B\theta' [\sinh(A_1 |R|)]^n \text{sgn}(R) \quad (2)$$

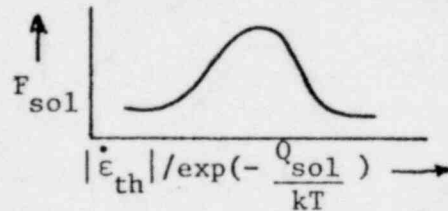
$$\dot{F}_{def} = H_2 [C_2 + |R| - (A_2/A_1) F_{def}^{1.5}] |\dot{\epsilon}_{th}| + H_3 \phi - H_2 C_2 B\theta' [\sinh(A_2 F_{def}^{1.5})]^n \quad (3)$$

$$F_{sol,1} = f_1(|\dot{\epsilon}_{th}|, T) \quad (4)$$

$$F_{sol,2} = f_2(|\dot{\epsilon}_{th}|, T) \quad (5)$$

$$\dot{\epsilon}_{irr} = B_2 \exp\left(-\frac{Q_{irr}}{kT}\right) (|\sigma/E|)^{n_2} (\phi)^P \text{sgn}(\sigma) \quad (6)$$

$$\dot{\epsilon} = \dot{\epsilon}_{th} + \dot{\epsilon}_{irr} \quad (7)$$

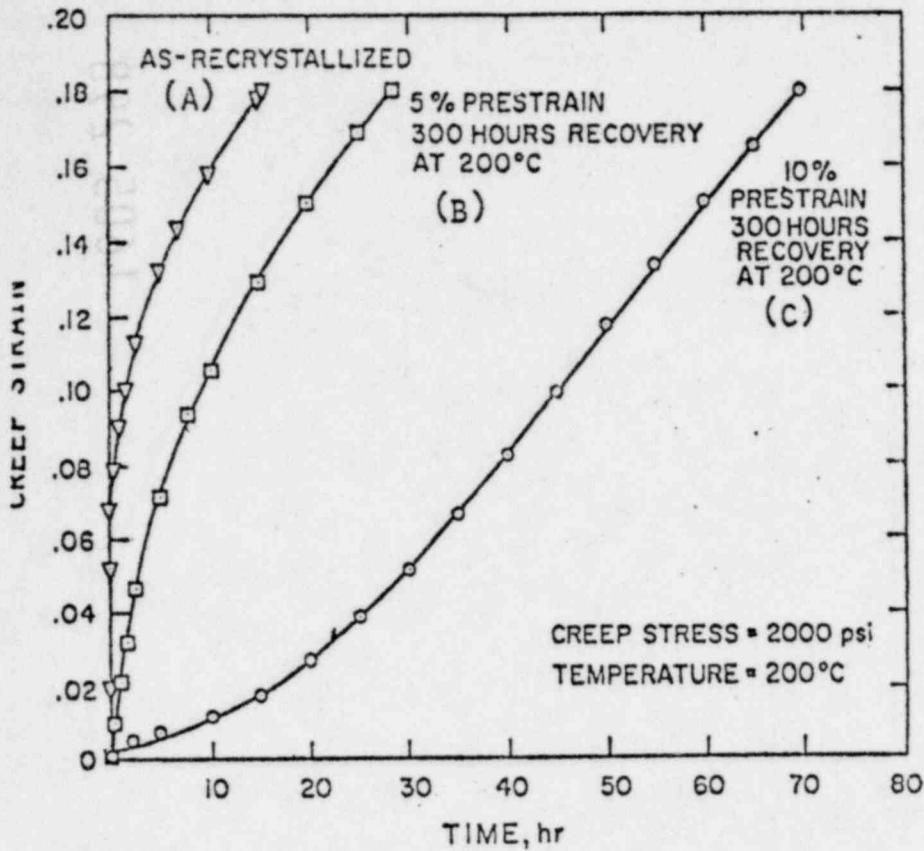


$\theta'$  is similar to  $\exp(-\frac{Q}{kT})$

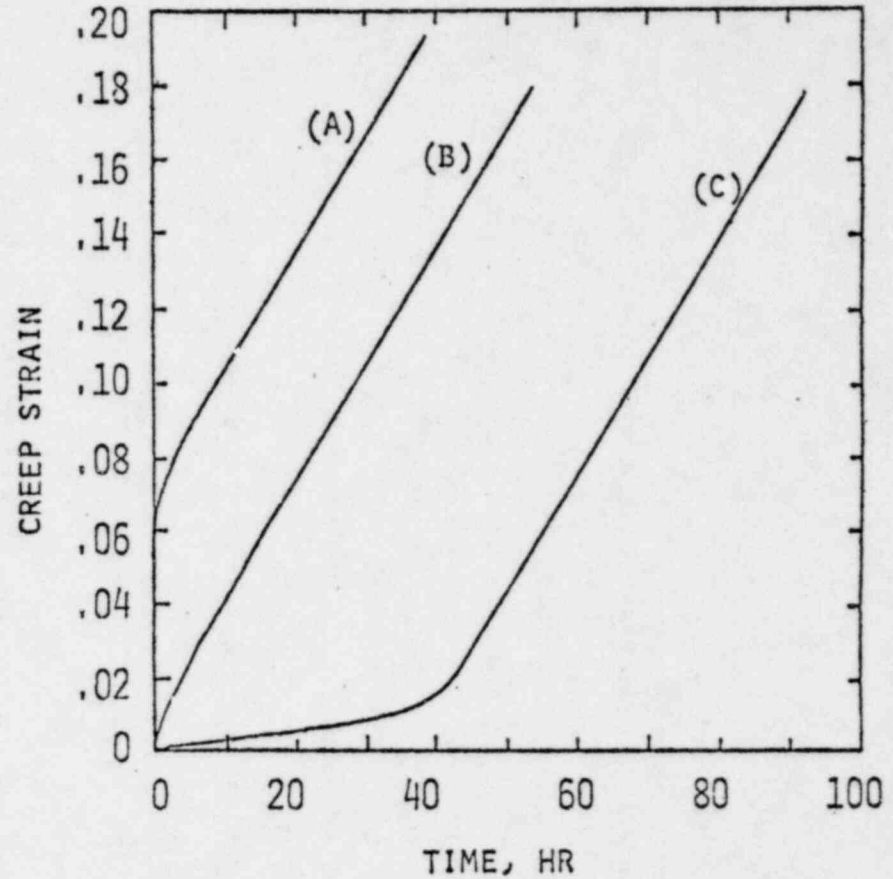
1605 298

Figure 1.

PURE ALUMINUM



(a) Data of Chen, Young, and Lytton [11]



(b) MATMOD simulations; curves A, B, and C are for the same histories and creep conditions as their experimental counterparts in Figure 8a.

Figure 2. Experimental data and independent simulations of the effect of prior room-temperature straining on the subsequent creep response. Prestraining reduces the amount of primary creep; the work hardening is not removed by static annealing at 200°C, but dynamic recovery occurs upon subsequent creep testing at 200°C.

1605 299

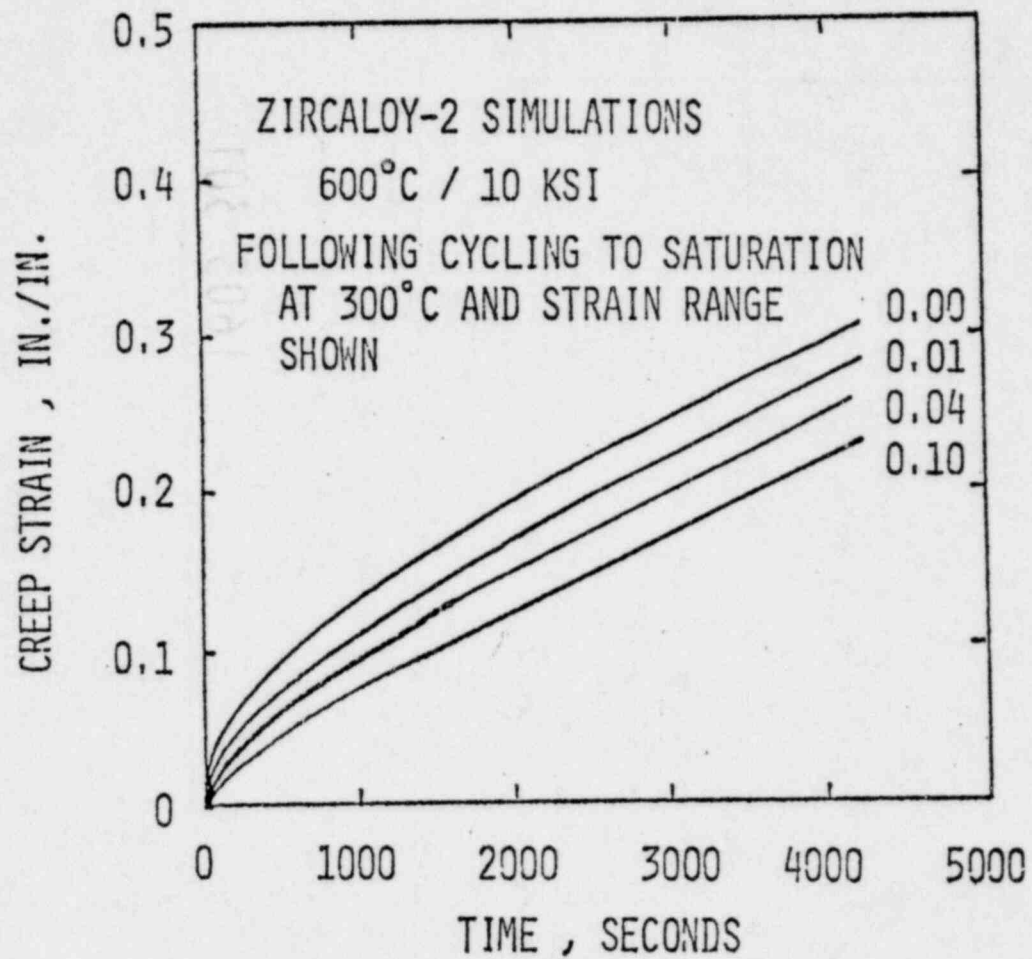
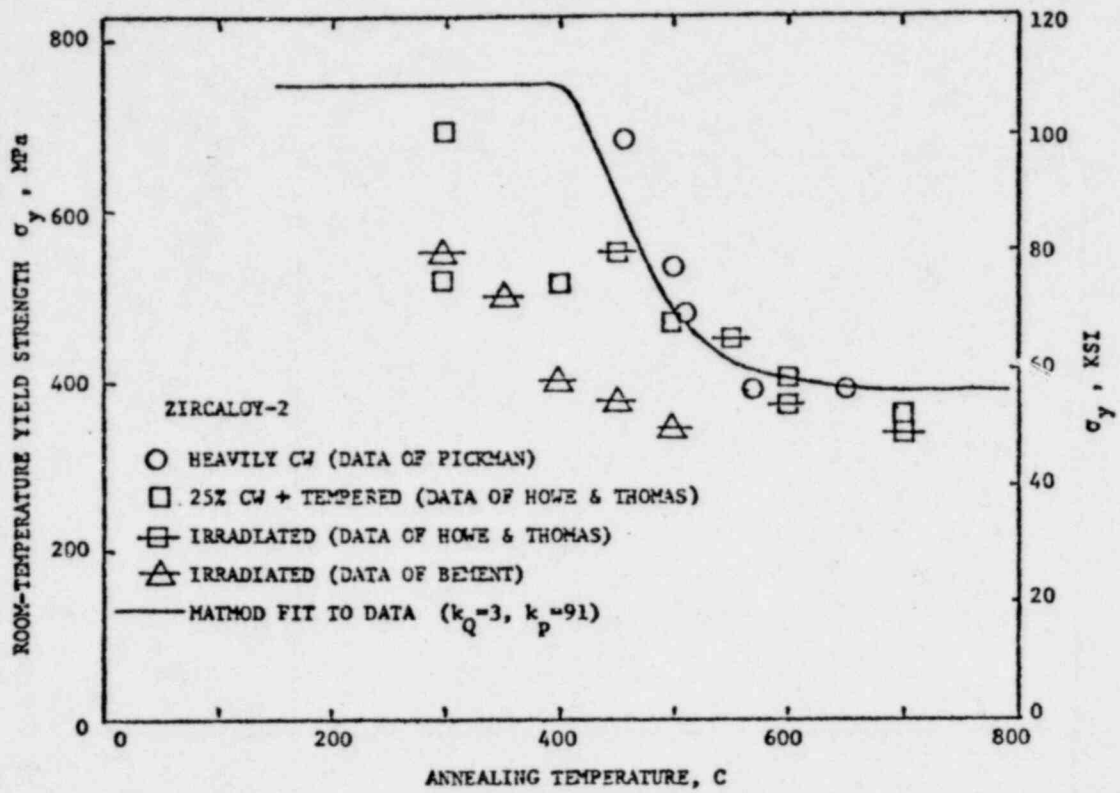


Figure 3. Simulations of the effect of prior cyclic straining on the subsequent creep response. Prior cycling reduces the amount of primary creep.

1605 500





1605 301

Figure 4.

1605 301

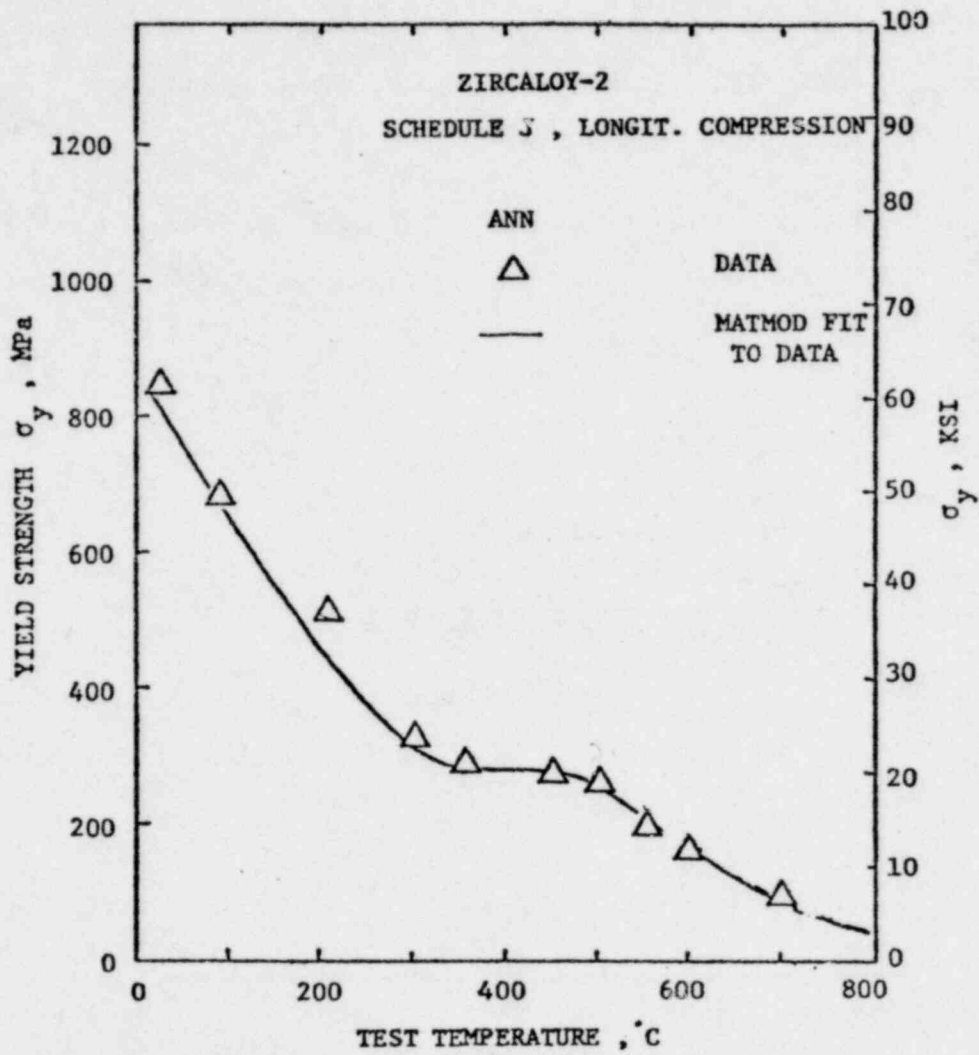


Figure 5.

1605 302

1605 302

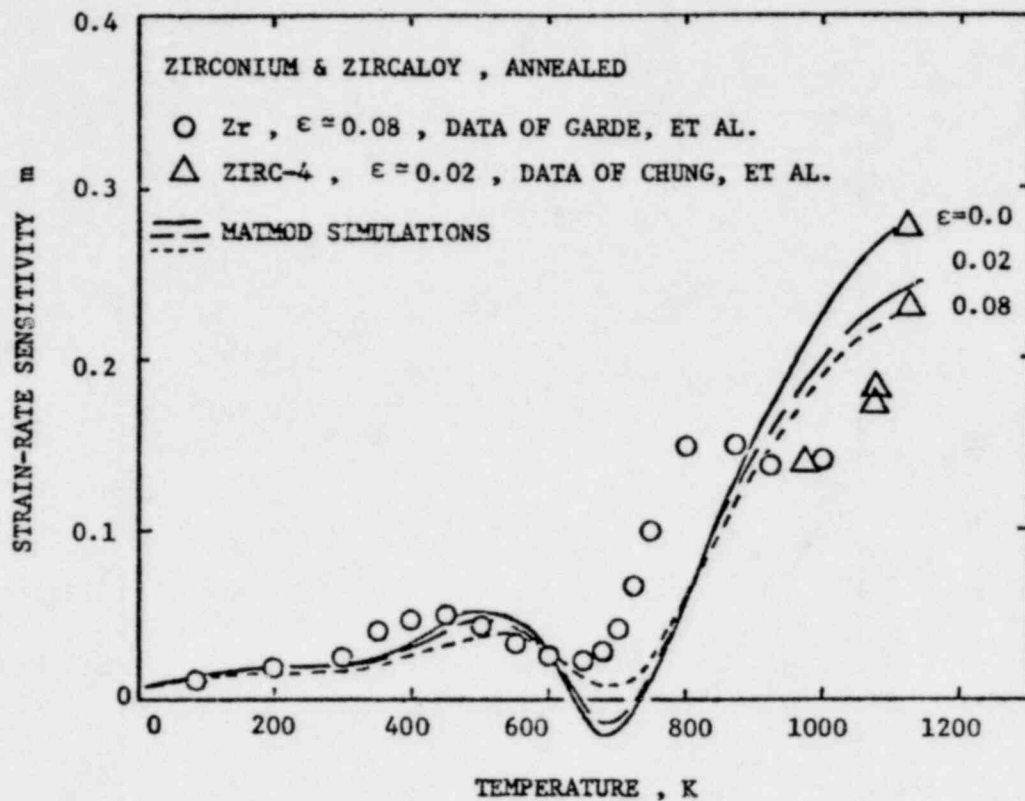
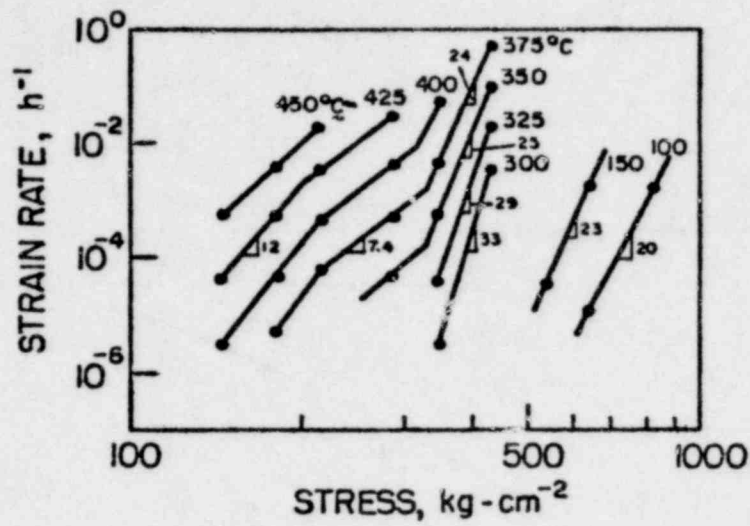
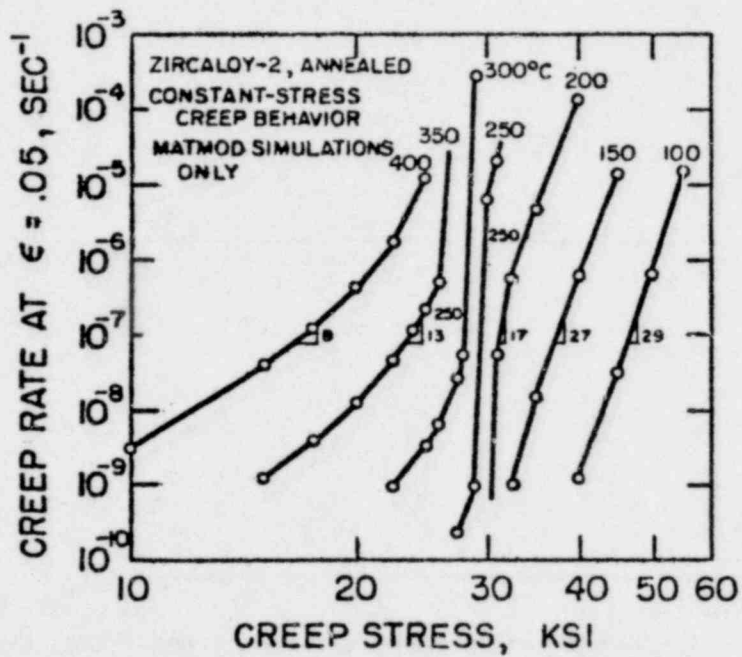


Figure 6. Strain-rate sensitivity as a function of temperature at various strain levels. The simulations utilize the final material constants and are independent of the data

1605 303



(a) EXPERIMENTAL DATA



(b) MATMOD SIMULATIONS

Figure 7.

1605 304

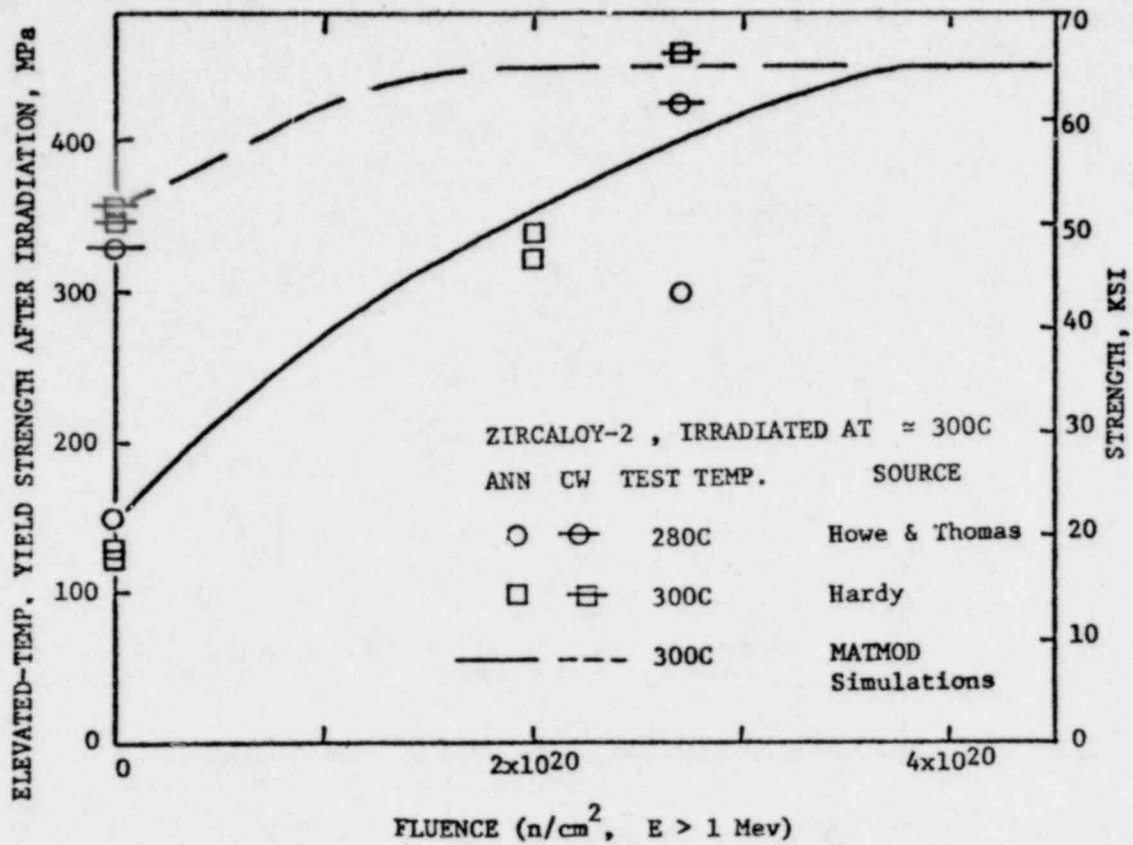


Figure 8. Elevated-temperature yield strength annealed and cold-worked material as a function of fast fluence. The simulations used the final material constants and (for fluences unequal to zero) are independent of the data [86,93].

1605 305



THEORY OF THE CREEP OF ZIRCALOY

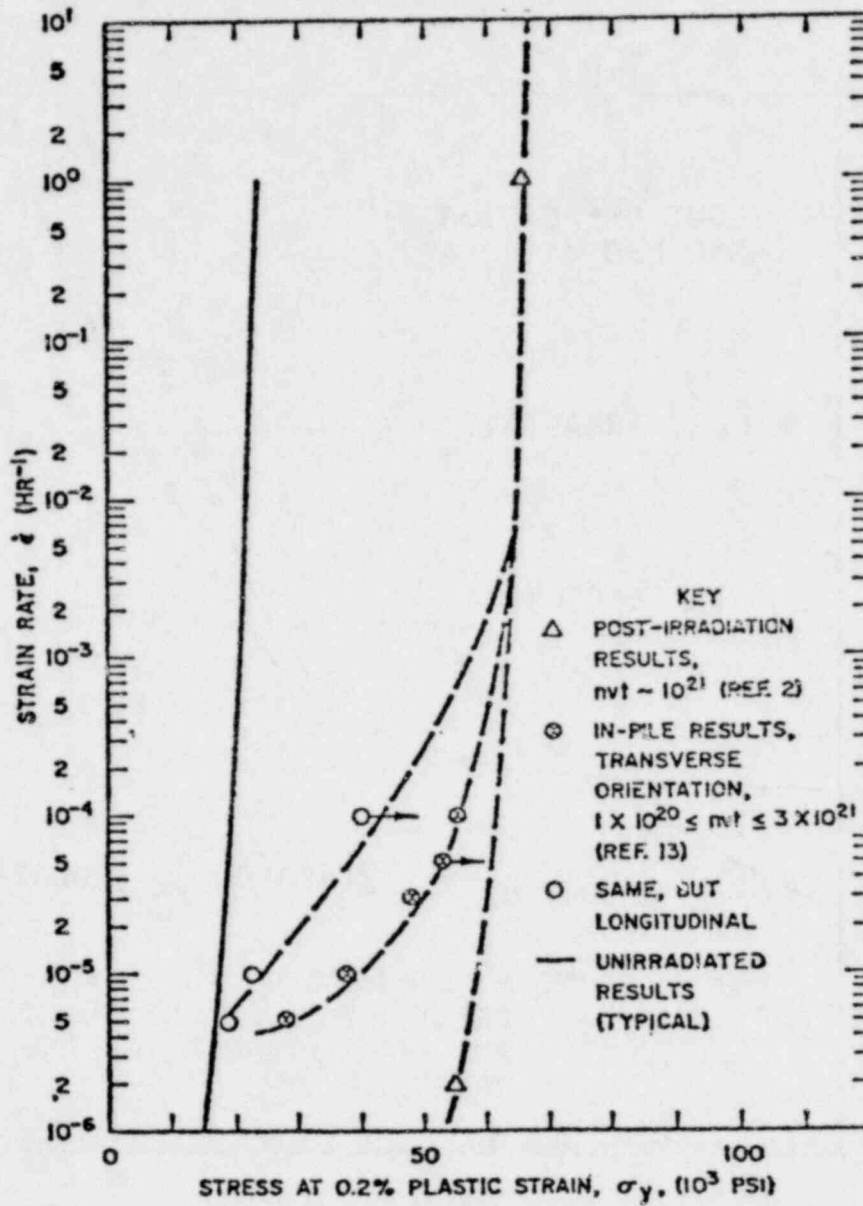
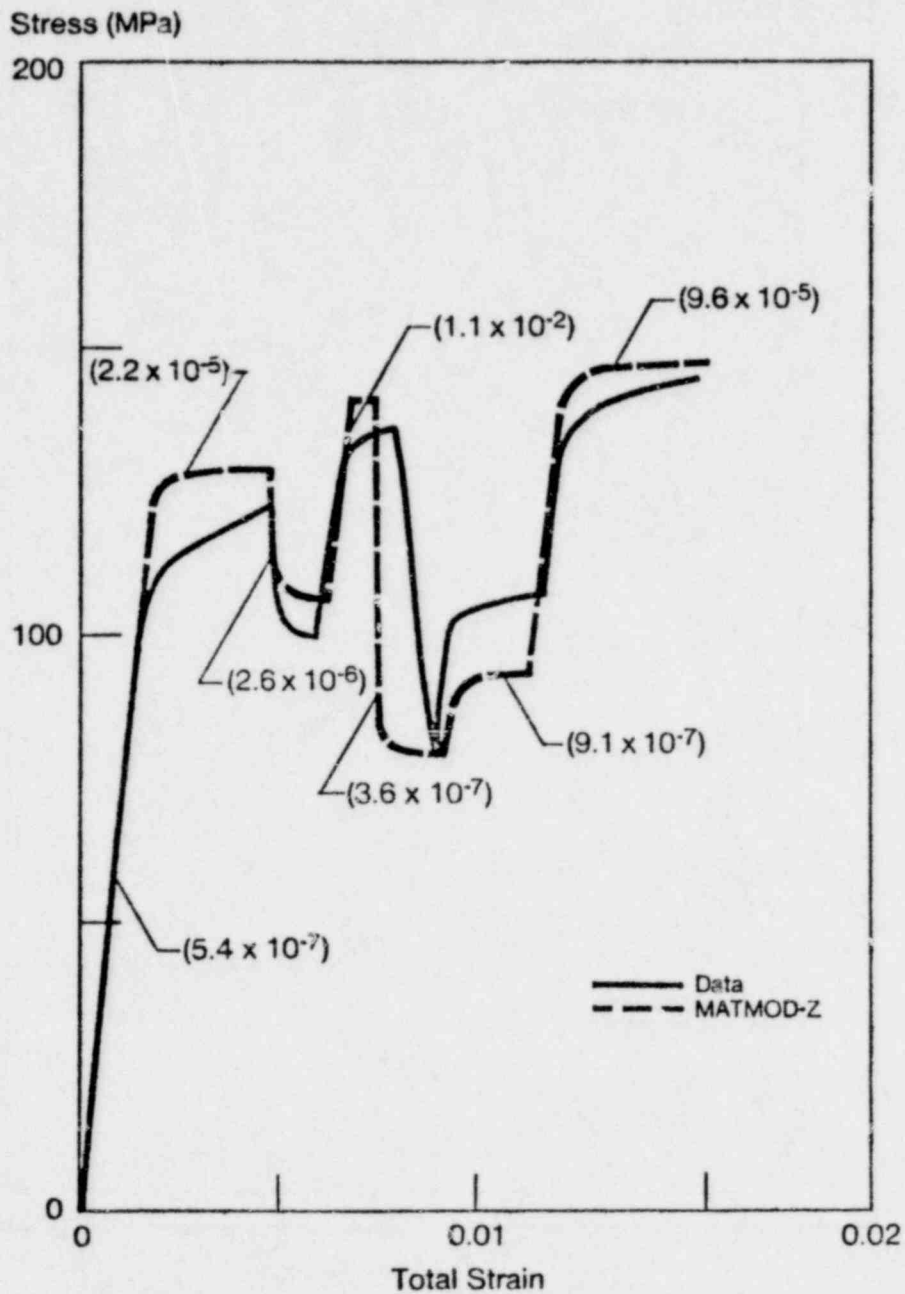


Figure 9b. Zircaloy data on in-reactor, out-of-reactor, and post-irradiation strain vs. stress, for comparison with simulation in Figure 9a.



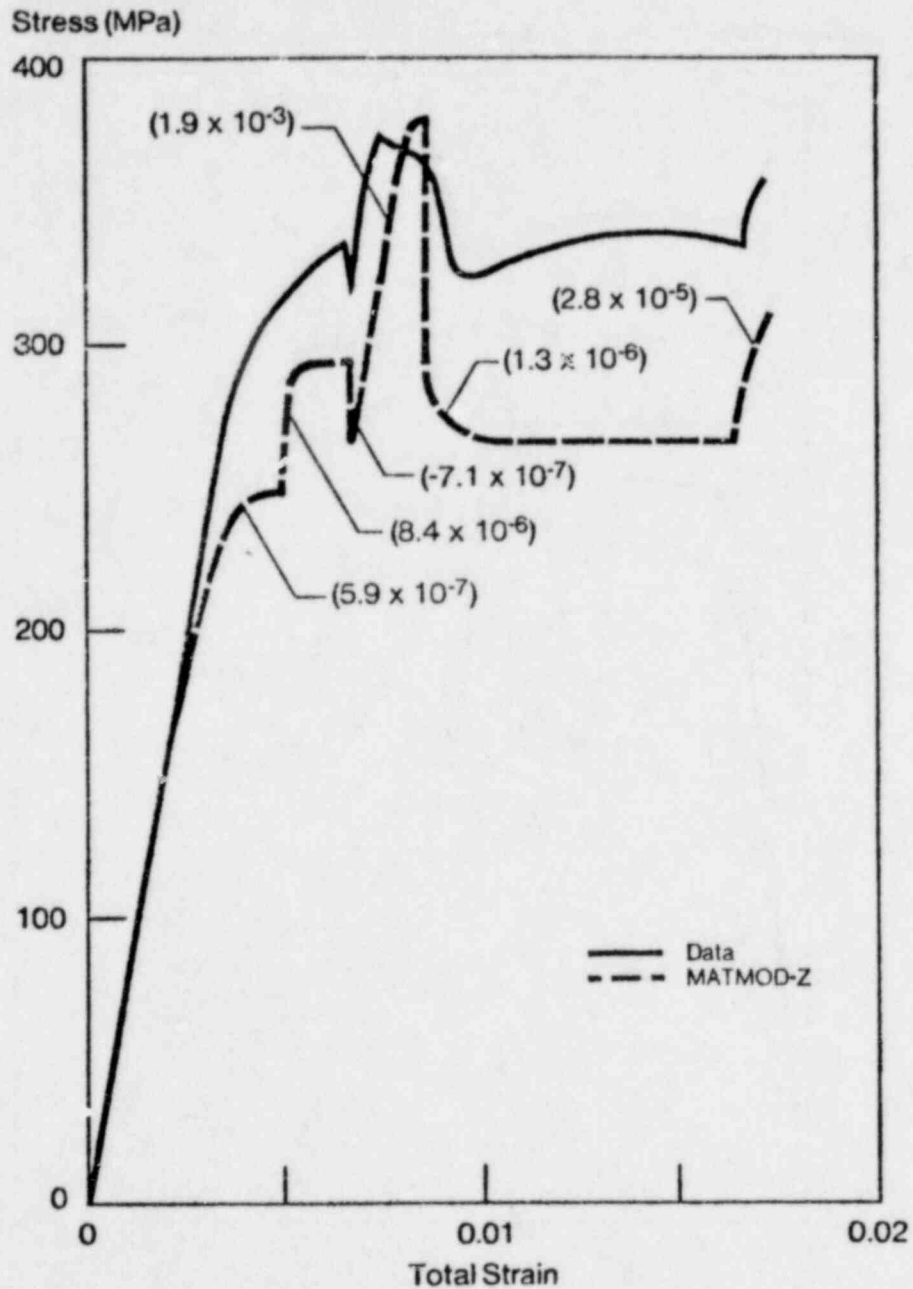
NOTE: Numbers in parentheses denote strain-rate ( $\text{sec}^{-1}$ )

Figure 10. Test  $\phi$ . Fully Annealed Zircaloy-2 Plate (Schedule J) Tested at  $450^{\circ}\text{C}$  in Transverse Direction.

1605 308

1605 308





NOTE: Numbers in parentheses denote strain-rate ( $\text{sec}^{-1}$ )

Figure 11. Test  $\alpha$ . Cold Worked and Stress Relieved Zircaloy-2 Plate (Schedule J) Tested at  $350^{\circ}\text{C}$  in Transverse Direction.

1605 309

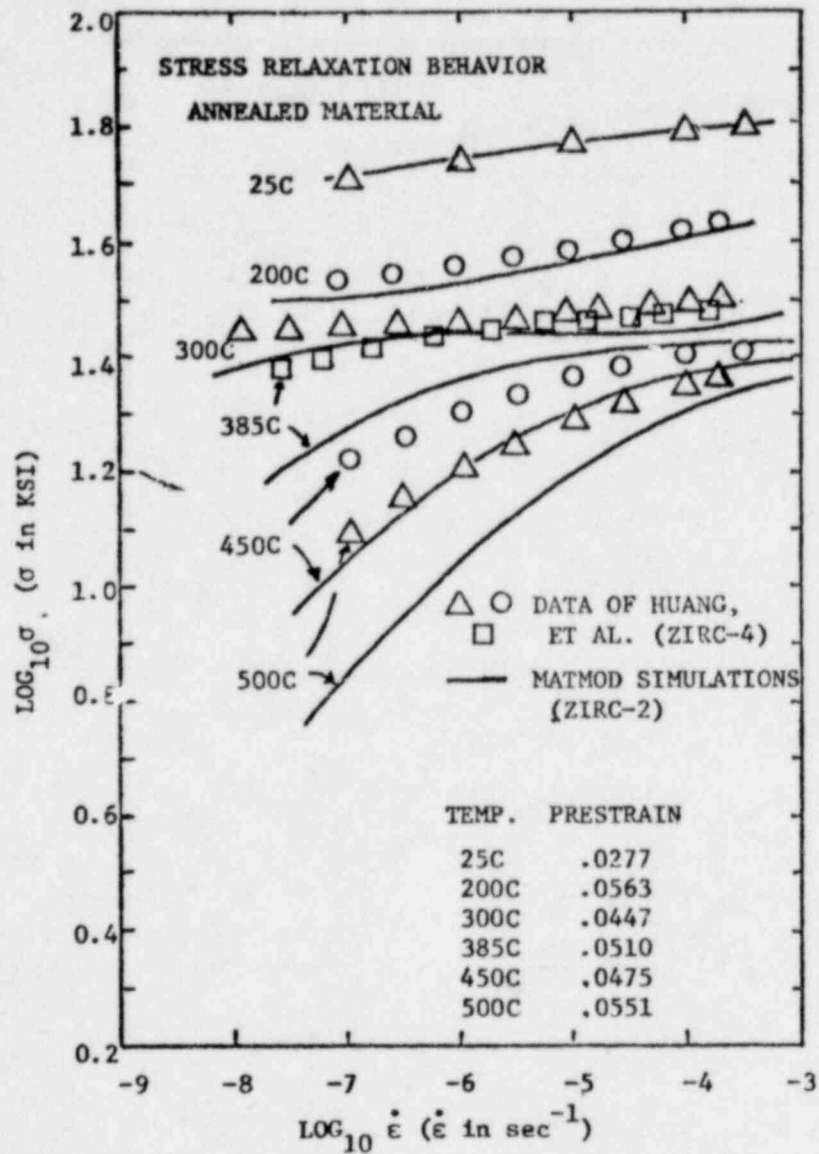


Figure 12. Stress relaxation behavior of annealed Zircaloy. The simulations (final material constants) are totally independent of the data

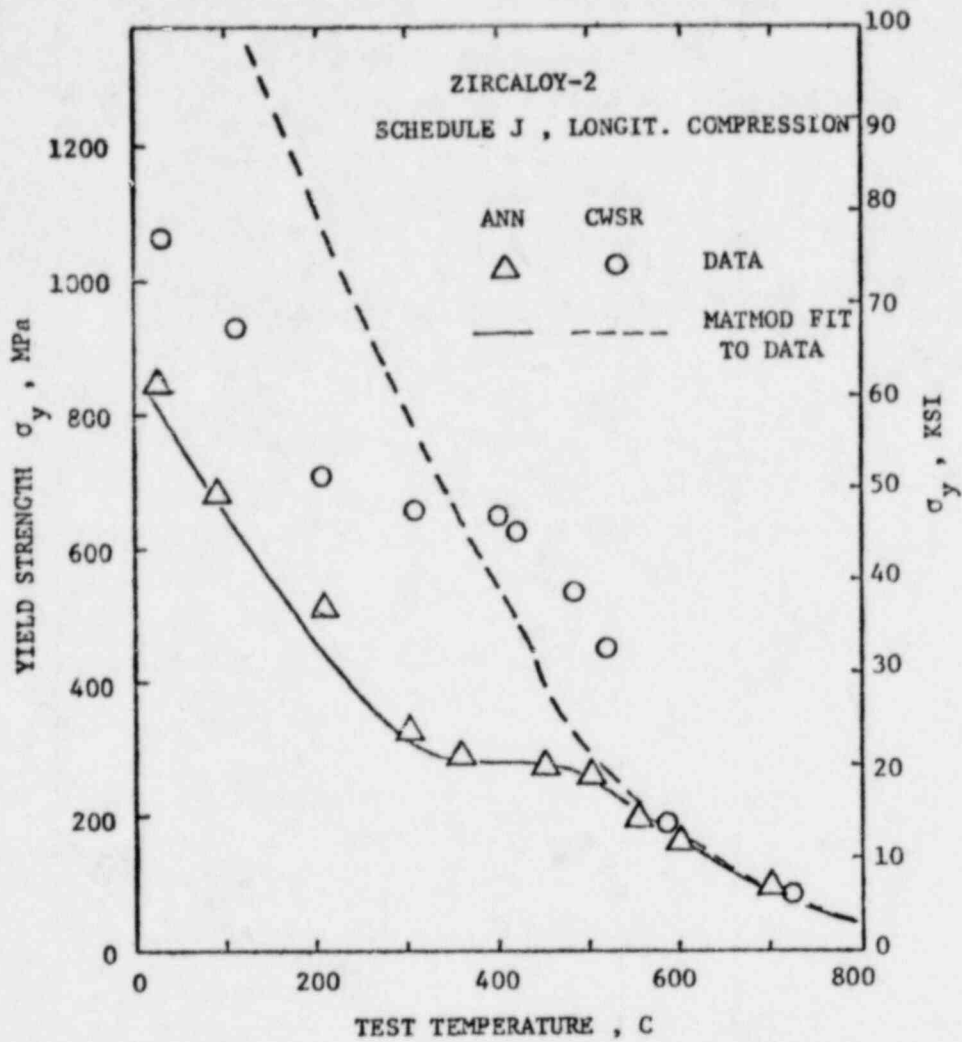


Figure 13. Yield strength as a function of temperature, for annealed material and cold-worked material. The simulations use the final material constants. Data from this research program (Appendix A).

1605 311

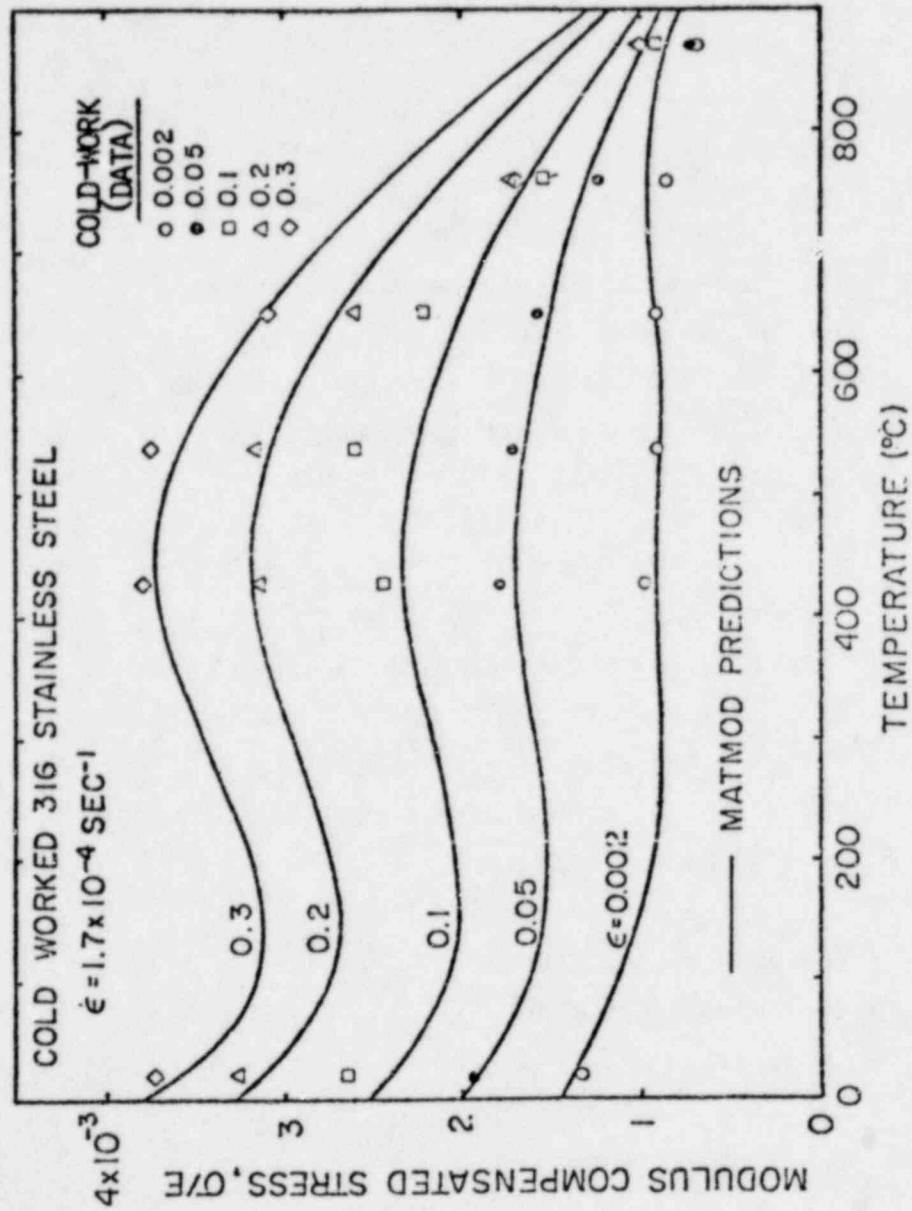


Figure 14. Yield strength (data and independent MATMOD predictions) for type 316 stainless steel cold-worked by various amounts.

1802 213

1605 312

Phenomena Simulated by the  
MATMOD Constitutive Equations

1. "Plasticity", including:
  - (a) essentially elastic behavior followed by gradual yielding
  - (b) strain-rate sensitivity
  - (c) temperature sensitivity
2. "Creep", including:
  - (a) primary creep
  - (b) steady-state creep
  - (c) sinh variation of steady-state creep rate with stress
3. Cyclic stress-strain behavior, including:
  - (a) Bauschinger effect
  - (b) cyclic hardening and cyclic softening
  - (c) shakedown to a saturated condition of constant stress and strain amplitudes
4. Recovery:
  - (a) static recovery
  - (b) dynamic recovery
5. Dynamic strain-aging effects, including:
  - (a) plateau in yield strength vs. temperature
  - (b) negative strain-rate sensitivity
  - (c) effect on creep rate
6. Complex histories:
  - (a) stress changes
  - (b) strain-rate changes
  - (c) temperature changes
7. Irradiation effects:
  - (a) irradiation hardening
  - (b) irradiation-enhanced creep
  - (c) channelling (strain softening)
  - (d) swelling
8. Interactions of all of the above

Figure 15.

1605 313